Survey of plasma crystal symmetry

N. BANU[a,b], D. TOADER[a,b], M. L. MUNTEANU[a], A. SCURTU[a,b], C. M. TICOŞ[a,c*]
[a]*National Institute for Laser, Plasma and Radiation Physics, 077125 Bucharest,Romania*
[b]*University of Bucharest, Faculty of Physics, 077125 Bucharest, Romania*
[c]*National Institute for Research and Development in Microtechnologies, 077190 Bucharest,Romania*

Plasma crystals are 3-D structures made of dust particles produced in laboratory low ionized gases. The confinement of the dust particles leads to self-ordering with symmetries which depend on gas discharge parameters, electrode geometry or dust particle features. A survey of plasma crystal symmetry observed in low pressure gas discharges is carried out.

(Received November 22, 2012; accepted September 18, 2013)

Keywords: Dusty plasmas, Crystal symmetry

1. Introduction

Dusty plasmas represent ionized gases which contain charged particles of matter. The presence of dust plays an important role in many fields of physics ranging from astrophysics, to the physics of atmosphere or industrial plasma research. Dust is an "old" problem in astronomy and astrophysics because of its presence in planetary rings [1], nebulae [2] or comet tails [3].

In the last decades there has been a growing interest in plasmas filled with dust particles. Surprisingly, dust in plasma appeared to be a critical issue in the development of microelectronics components [4]. Breaktroughs in material science and nanotechnology often depend on the contamination of the processing plasma with even very small particles. Other areas showing increased interest in dusty plasmas are solar cell [5] and catalysts industries[6]. Initially, the technological processes were more focused on removal of the dust, which grows in glow discharges. Later it has been shown that the incorporation of nanometer-sized dust particles in the substrates can substantially increase the performance of materials [7-8]. Moreover, a cloud of microparticles present in plasma can scatter eficiently the electromagnetic waves in the optical, IR or even THz range [9].

The possibility of forming Coulomb crystals in glow discharge filled with dust was initially put forward by Ikezi in his simple theoretical prediction [10]. Several years later Coulomb crystals were observed in experiments [11-12]. The relatively easy and afordable diagnostics, which are required for the investigation of the Coulomb crystals make them an ideal system to study the structure and dynamics of finite charged-particle systems at a convenient time and space scale.

2. Forces acting on dust particles

In plasma the mobility of the electrons is much larger than that of ions. This can lead to a charge separation which generates an electric field especially at the plasma-wall boundary in the case of a plasma produced in the laboratory. This electric field accelerates the ions towards the walls, giving rise to a sheath. In the plasma sheath the density of electrons rapidly decreases to zero [13].

A microparticle immersed in plasma is charged negatively. The fluxes of ions and electrons to the dust surface eventually reach an equilibrium and the resulting dust potential is negative relative to the surrounding plasma potential [14].

The dust particles present in plasma are subjected to several forces. Depending on the experimental conditions, some of these forces are dominant or other ones can be neglected.

The Force of Gravity. In most experimental (and numerical) cases, especially when the features of crystal structures are under study, spherical dust particles are considered. The gravitational force is then:

$$\vec{F}_g = m_p \vec{g} = \frac{4}{3}\pi r_p^3 \rho_d \vec{g} \quad (1)$$

where m_p is the dust particle mass, $\vec{g}$ is the gravitational acceleration, r_p is the particle radius and ρ_d is the dust particle mass density. It can be seen that the gravitational force has a cubic dependence on the particle.

The Electric Force. In the presence of an electric field E, the force acting on a charged dust particle is

$$\vec{F}_e = Q_d \vec{E} \quad (2)$$

were Q_d is the dust particle charge.

This force can cause the trapping of the dust particles in plasma. In the sheath near the electrode the electric force acts against the force of gravity, and dust grains can be levitated on the account of a balance between these two forces. Near the electrode, the sheath potential profile $V_{sh}(z)$ can be approximated as parabolic [15], and therefore $E_{sh}(z) = -dV_{sh}/dz$ is roughly linear far from the plasma-sheath edge.

The Neutral Drag Force. When a particle is moving inside the plasma, it experiences a force of resistance from

the surrounding medium, i.e. the neutral gas. The neutral drag force is proportional to the velocity of the particle relative to that of the fluid and depends quadratically on the particle radius. The neutral drag force when the dust speed is low is

$$F_{dn} = -\frac{8}{3}\sqrt{2\pi}r_p^2\, n_n v_{tn}(v_d - v_n) \qquad (3)$$

where n_n is the density of the neutral gas, v_d is the dust particle speed, v_{tn} is the thermal gas speed, and v_n is the speed of the gas flow [16]. The neutral drag force is particularly important for dissipation of the dust kinetic energy through friction with the gas atoms and condensation into a crystal.

The Ion Drag Force. Experiments and numerical investigations have showed that the ion drag force acting on dust grains in plasmas plays an important role in dust structure formation, dust-dust interactions, or in technological problems such as removal of dust which grows in glow discharges.

The most studied case is when the dust radius is much smaller than the debye length [17-18]. The ion drag force has two components: the direct impact force and the long range Coulomb force.

The thermophoretic force. An analytical expression for the thermophoretic force is given by [19],

$$F_{th} = -\frac{32}{15}\frac{r_p^2}{v_{tn}}\left[1 + \frac{3\pi}{32}(1-\alpha)\right]k_T\nabla T_n \qquad (4)$$

where α is an accomodation coefficient, k_T is the thermal conductivity of the gas and ∇T_n is the neutral gas temperature gradient. The thermophoretic force has a quadratic dependence on the particle radius as well. The use of the termophoretic force by heating the electrode of the discharge has led to the observation of spherical dust structures also called Coulomb balls [20].

The radiation pressure force. Imaging of dust particles is possible due to the use of a laser beam of a few mW which illuminates the particles. When the flux of photons reaching the surface of the particles is high enough, the laser beam can push the particles around. Radiation pressure is the momentum transferred by photons on any unit area surface exposed on unit time. According to [21] the radiation pressure force is given by:

$$F_{laser} = \gamma\frac{n_1\pi r_p^2 I_{laser}}{c} \qquad (5)$$

were γ is a dimensionless factor determined by the reflection, transmission and absorption of the particle, n_1 is the refractive index of the gas around the particles, c is the speed of light and I_{laser} is the intensity of laser. A quadratic dependence exists between the radiation pressure force and particle radius. Since the strength of external forces acting on dust particles is important for levitating the particles and obtaining a stable crystalline structure, a summary is presented in Table 1 which gives the dependence of these forces with the radius of a dust particle. In most experimental cases the first (i.e. gravity) and the last (i.e. electric) forces are dominant.

Tabel 1. Dependence of external forces on dust particle size

Name	Size dependence
The force of gravity	r_p^3
The neutral drag force	r_p^2
The ion drag force	r_p^2
The radiation pressure force	r_p^2
The thermophoretic force	r_p^2
The electric force	r_p

2.1 Charging of dust

Dust particles immersed in plasma aquire electrical charges and constitute an additional charged plasma component besides electrons and ions. The dust particle charge is determined by the local plasma parameters, which can vary both temporally and spatially. The large inertia of a dust particle makes it insensitive to changes at temporal scale of a few MHz such is the case in RF plasma. However, a slow temporal variation of a few Hz of the electrode potential can easily induce dust charge modifications and lead to dynamical changes in the equilibrium of dust particles.

Electron and ion fluxes to the particle surface are determined by the integration of the corresponding cross sections with velocity distribution functions [16]. If a Maxwell-Boltzmann distribution is considered the electron and ion currents from background plasma are:

$$I_e = \sqrt{8\pi}r_p^2 n_e\, v_{T_e} exp\left(\frac{eV_d}{k_B T_e}\right), \qquad (6)$$

$$I_i = \sqrt{8\pi}r_p^2 n_i\, v_{T_i} exp\left(1 - \frac{eV_d}{k_B T_i}\right), \qquad (7)$$

where $n_{e(i)}$ is the electron (ion) number density, $v_{T_{e(i)}} = \sqrt{\frac{k_B T_{e(i)}}{m_{e(i)}}}$ is the electron (ion) thermal velocity and V_d is the dust potential, with $V_d < 0$.

The charging equation is:

$$\frac{dQ_d}{dt} = I_e + I_i.$$

An equilibrium dust potential is reached when $I_e = I_i$. A perfect dust sphere is considered to act as a spherical capacitor and its charge is given by $Q_d = 4\pi\varepsilon_0 r_p V_d$.

The electric charge carried by the dust particles leads to a high electrostatic energy of interaction between particles comparable to their kinetic energy. The strong electrostatic coupling in the dust system can favour the appearance of short-range order and even crystallization. According to [23] the first experimental realization of the

ordered (quasi-crystal-like) structure of charged microparticles in a neutral gas was obtained by Wuerker et al. [24] in 1959.

2.2 Formation of Coulomb Crystals in plasmas

When the weight of a dust particle is compensated by some other forces such as the electric force or the termophoretic force, the charged particle can be levitated inside the discharge [14,16].

Trapping of a dust particle cloud in a localized region of the discharge is usually realized by an electrostatic confinement which prevents dust to drift away pushed by the Coulombic forces. The confinment is realized in rf plasma by placing a ring on the electrode. In a dc discharge the particles are trapped in the anode glow or in the positive column [23].

Experimentally, the ordered structures of dust particles were first observed near the sheath edge of rf discharges [11-12,15, 20-21, 25-35].

It appears that the combined action of Coulomb repulsion, neutral drag force and ion wake force play an essential role in the formation of the dust crystal 3-D structures. The fist one insures a regular horizontal spacing while the second one dissipates the excess kinetic energy of particles. Finally, the third one leads to a vertical alignment of the dust particles, where the grains are on top of each other in a string-like arrangement.

Experimental setups. Dusty plasma crystals have been discovered in 1994, simultaneously by H.Thomas et al. and by J.H. Chu et al. [11-12]. Since then many laboratories have been actively involved in the investigation of crystal properties, from structural features to phase transitions, dynamics and aggregation of dust particles.

The details about the structure of plasma cristals under various experimental conditions. are given in Table 2.

In the case of rf dusty plasmas the experimental setup included in most cases a lower electrode which had different shapes such as disks [11,28-29], ring-shaped groove in a disc [12, 34], disc provided with a depression [28] or cylinder [33] coupled to an rf generator with a frequency of 13.56MHz [11,20-32] or 14MHz [12,33] and an upper grounded electrode. The grounded electrode has also been used in different shapes: disc with a circular cut [11,25] ring [17, 34], or a wide mesh grid [29].

A somewhat different configuration was present in the experiments of Bouchoule et al. [8] where the top electrode was rf driven while the bottom was a gride grounded electrode, and in those of Lin I et al. [33] where the bottom electrode was grounded and the rf was a cylinder.

The two electrodes were placed into a vacuum discharge chamber provided with optical windows on the side and at the top. The crystals could thus be imaged along two orthogonal directions, from the side and from the top.

The dust particles were immersed in plasma with a dust dispenser usually through a wire mesh [30,35], or a cylinder under vacuum which was provided with a dust cup [36].

In order to image the dust cloud, the microparticles were illuminated by a laser sheet. It was obtained by passing an expanded circular beam through a cylindrical lens with focal length f~5-25 cm. It was thus possible to produce a flat sheet laser beam with thickness of the order of 100-300 microns and only a plane (horizontal or vertical) of the crystal could be selectively illuminated [11,12, 20, 25-36].

The dust particles and gases used. In most experiments spherical grains were used. Particle symmetry greatly simplifies the study of forces acting on the particles, and often allows to consider the dust particles as point-like objects.

From a theoretical point of view, the charging mechanism of a dust grain with irregular shape is difficult to model and involves many approximations. Nevertheless, non-spherical dust grains can be found in space, in fusion devices, in industrial applications and in laboratory experiments as well.

Particle diameters usually lie in the range from 1 [33] to 10 [12] μm. In principle dust particles with larger sizes can be levitated as long as their weight permits it. Hollow particles are lighter and can reach diameters of tens of microns. As can be seen in Table 2 the most used particles were made of melamine formaldehyde which is a special type of resin with low density (1.5 g/cm^3), available as powder of perfect spheres from commercial suppliers. In their work Pieper at al. have also obtained 3D Coulomb crystals using polymethylene melamine particles with 9.4 μm in diameter [28]. Hayashi have used carbon particles with a diameter of 1.4 μm which were formed inside the discharge [20]. Ordered structures were also observed for TiO_2 [32], SiO_2 [12,33] or even glass particles [37].

In most cases inert gases were pumped inside the plasma chamber. The pressure ranged from a few mTorr to well over 1 Torr. The used gases were Argon [11,12,20-27], krypton [28-30], helium [31] or different mixtures [12,26,33] incorporating reactive gases such as SiH_4, O_2 or CH_4 wich would lead to the formation of dust particles inside the chamber, which have grown in time by coagulation, from a few nanometers to several microns.

2.3 Symmetry of plasma crystals

In a range of pressure and rf power, as given in Table 2, the dust particles forming a cloud come to rest. In spite of their initial positions they do not spread randomely but rather self-organize into a regular structure with the interparticle distance having a tendency to take some specific values. The interparticle distance can be inferred from the pair correlation function [23]. The crystal is stable in time as long as the discharge parameters are kept relatively constant. Aligmnent of the charged dust particles inside the confining region takes place over all three spatial directions. The horizontal layers are filled with particles symmetrically disposed in a hexagonal or in the case of a mutilayer crystals in a hexagonal closed-packed (hcp), a body-faced-centered (bcc), or a face-cubic-centered (fcc) configuration [11,12,20,25-35]. The

hexagonal and hcp have been however reported in most experiments, except in a C-filled dusty plasma produced in argon and methane [26], where a face-centered orthorombic (fco) configuration has been observed.

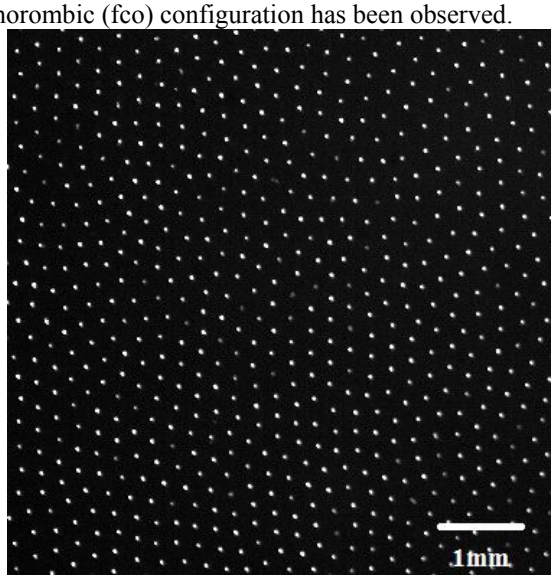

Fig. 1 Horizontal layer in a plasma crystal

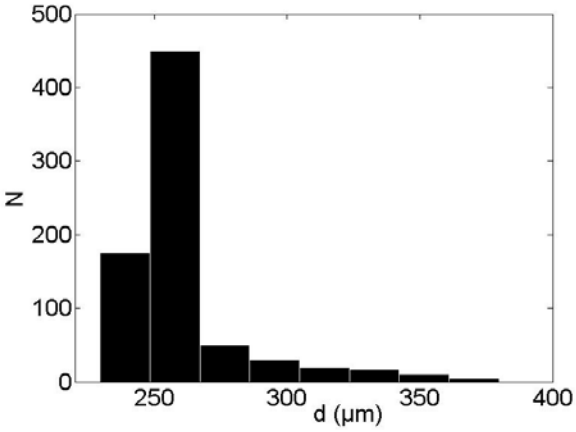

Fig. 2 Distances between dust particles in a horizontal plasma crystal plane.

A typical hcp simmetry is shown in Fig. 1 where the top horizontal layer of a plasma crystal is shown. The crystal was produced in argon between parallel plates electrodes using a confining potential well created by a cut in the lower electrode with a depth of 1.5 mm. The pressure was 300 mTorr while the rf signal applied on the electrodes had 3 W at 13.56 MHz. The particles in the figure have 6.02 μm in diameter. The average lattice size in the arrangement of Fig. 1 is about 260 μm, as shown in Fig. 2. Here a histogram of the distances between the imaged dust particles is presented. The hexagonal symmetry within the plasma layer is better evidenced in Fig. 3 which shows a Wigner-Seitz cell analysis of the dust particles.

The hexagonal symmetry in a crystal is not singular and often coexists with bcc and fcc structures, even in microgravity conditions where interaction between the dust particles is supposed to be almost isotropic [30,35]. Whereas the bcc and fcc are lower free energy states, the hexagonal is mostly encountered in experiments due to the local conditions for crystal formation where the ion flow plays an important role.

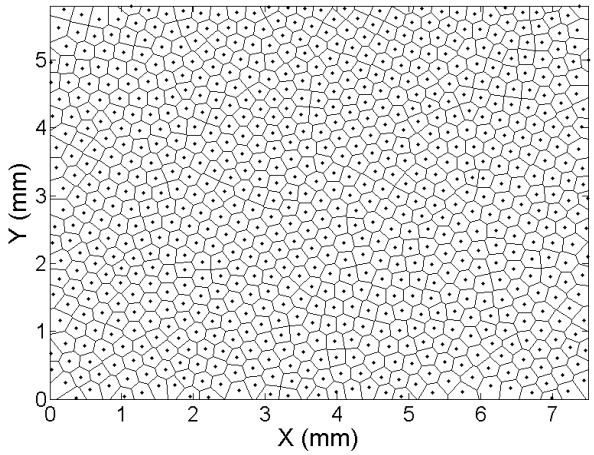

Fig. 3 Voronoi diagram of dust particles in a horizontal lattice plane

Thus, in pure argon or combined with silane and oxygene bcc and fcc were simultaneously observed with hcp symmetry [12,27-28,33,35].

The ordering of the microparticles does not seem to depend on the type of gas, particle size or level of rf power. Crystals with hcp symmetry have been produced in a large range of discharge conditions, at lower pressures (few mTorr) and low rf power levels (below 1W) [30] to hundreds of mTorr and tens of Watts [12,32]. In some cases however, plasma crystals can be formed at relatively higher gas pressure (1.4 Torr) in Krypton [28]. The lattice size seem to vary depending on experiments from 195 μm [28] to 720 μm when similar plastic particles are used [34], and can go up to 880 μm for TiO_2 particles [32].

3. Conclusions

A survey of experimental conditions for producing dust crystals in plasma has been presented. The common parameters and discharge features have been discussed in close connection with the observed symmetry of the crystals. Most experiments reporting on plasma crystals have been performed in rf discharges. It was found that the hexagonal symmetry prevails, probably due to the peculiarities of the ion flow inside the sheath which favour the vertical aligment of the dust particles. Other arrangements such as bcc and hcp have been observed as well. The crystal symmetry could play an important role in future applications of plasma crystals related to light or electromagnetic wave scattering.

Acknowledgements

N. Banu, D. Toader, M.L. Munteanu, and A. Scurtu were supported by the National Authority for Scientific Research (ANCS) from contract Nucleu-LAPLAS 2012. C.M.Ticoş acknowledges support provided by the Sectoral Operational Program Human Resources and Development (SOP HRD) financed from the European Social Fund, and by the Romanian Government under contract POSDRU 89/1.5/*S*/63700.

Table 2. Symmetry of plasma crystals, parameters of the discharge and features of the dust particles in rf plasmas. In a few references some plasma parameters are not available (na).

Particle diameter (μm)	Material	Lattice type/ intergrain distance (μm)	Number of crystalline layers (shells for spherical)	P(mtorr)/ gas	Vp-p for rf/ or Vdc (V)	Power (W)/ dc or rf	Reference
7±0.2	MF	hcp/ 250	18 layers	1.5±.038/ argon	Na	4.5±0.2/rf	[11]
10	SiO_2	hcp, bcc, fcc/200	na	10-200/ argon +O_2, SiH_4	Na	1-30/ rf (14 MHz)	[12]
3.4	MF	hcp/ 715	4 shells	350-1150/ argon	40-60	na/rf	[20]
6.5±0.3	MF	hexagonal/ 825	1	5/ argon	49	na/rf	[25]
1.4±0.05	C	fco/ 106-162	≥8	300/ argon and 20% methane	Na	5/rf	[26]
3.375± 0.102	MF	hcp+bcc,hcp+fcc/ 215	19	352/ argon	61.8V	na/rf	[27]
9.4±0.3	PEM	bcc and simple-hcp/ 195	1	1400/ krypton	200 and -43V p-p	2.3/rf	[28]
8.9±0.1	MF	hexagonal /256	1	40/ krypton	Na	50/rf	[29]
14.9	MF	300	3D	300/ krypton	Na	0.045-0.2/rf	[30]
9.4±0.3	MF	hcp	450/1	772-885/ helium	80-180	10-60/rf	[31]
0.1-30	TiO_2	hexagonal/ 880	na	560/ argon	55	5-30/ rf	[32]
~1	SiO_2	bcc, fcc, and hcp/~200	3D	200/ argon, O_2+SiH_4	Na	1/ rf (14 MHz)	[33]
8.9±0.1	plastic	hexagonal/ 550-720	1	15/ argon	Na	10/rf	[34]
3.4 and 6.8	MF	bcc, fcc, hcp/ 246-258	3D	75-750/ argon	Na	0.3/rf	[35]

References

[1] C. K. Goertz, Rev Geophys **2**, 271 (1989).
[2] A. G. W Cameron. and M.B. Fegley, Icarus **52**, 1 (1982).
[3] D. A. Mendis, in Advances in the Physics of Dusty Plasmas, Ed. P.K. Shukla et al., World Scientific Singapore,1997.
[4] G. S. Selwyn, J.E. Heidenreich, K.L. Haller, Appl. Phys. Lett. **57**, 1876 (1990).
[5] A. Bogaerts, E. Neyts, R. Gijbels, Mullen, Spectrochim. Acta Part B, **57,** 609 (2002).
[6] F. Nastase, I. Stamatin, C. Nastase, D Mihaiescu, A. Moldovan, Progr. Solid State Chem. **34**, 191 (2006).
[7] A. Drenik, R. Clergereaux, Mater. Technol **46**(1), 13 (2012).
[8] A. Bouchoule, A. Plain, L. Boufendi, J. Blondeau, C. Laure, J. Appl. Phys. **70**, 1991(1991).
[9] S. Ebbinghaus, K. Schröck, J. C. Schauer, E. Bründermann, M. Heyden, G. Schwaab, M. Böke, J. Winter, M. Tani andM Havenith, Plasma Sources Sci. Technol. **15**, 72 (2006).
[10] H. Ikezi, Phys. Fluids **29**, 1764 (1986).
[11] H. Thomas, G. E. Morfill, V. Demmel, J. Goree, B. Feuerbacher, D. Möhlmann, Phys. Rev. Lett. **73**, 652 (1994).
[12] J. H. Chu, Lin I, Phys. Rev. Lett., **72**, 4009 (1994).
[13] F.F. Chen, Introduction to Plasma Physics and Controlled Fusion, vol. 1, 2nd ed,Springer 1984.
[14]T. Nitter, Plasma Sources Sci. Technol. **5,** 93 (1996).
[15] E. B. Tomme, D. A. Law, B. M. Annaratone, J. E. Allen, Phys. Rev. Lett **85**, 2518 (2000).
[16] P.K. Shukla, A.A. Mamun, Introduction to Dusty Plasma Physics, IoP 2002.
[17] M. S. Barnes, J. H. Keller, J.C. Forster, J.A. O'Neill, D.K. Coultas, Phys. Rev. Lett. **68**, 313 (1992).
[18] S. A. Khrapak, A. V. Ivlev, G. E. Morfill, H. M. Thomas, Physical review E **66**, 046414 (2002).
[19] L. Talbot, R.K. Cheng, R.W. Schefer, D.R. Willis, J. Fluid Mech., **101**(4), 737 (1980).
[20] O. Arp, D. Block, A. Piel, A. Melzer, Phys. Rev. Lett. **93**, 165004 (2004) .
[21] Bin Liu, J. Goree, V. Nosenko, and L. Boufendi. Phys. Plasmas, **10**(1), 920 (2003) .
[22] P. K. Shukla, Reviews of modern Physics, **81**(1), 25 (2009).
[23] V. E. Fortov, A. G. Khrapak, S. A. Khrapak, V. I. Molotkov, O. F. Petrov, Phys. Usp. **47**, 447 (2004).
[24] R. F. Wuerker, H. Shelton, R.V. Langmuir, J. App. Phys., **30**(3), 342 (1959).
[25] S. Nunomura, D. Samsonov, J. Goree, Phys. Rev. Lett. **84**, 5141 (2000).
[26] Y. Hayashi,Phys. Rev. Lett. **83**, 4764 (1999).
[27] M. Zuzic, A.V. Ivlev, J. Goree, G. E. Morfill, H. M.Thomas, H. Rothermel, U. Konopka, R. Sutterlin, and D. D. Goldbeck,Phys. Rev. Lett. **85**, 4064 (2000).
[28] J. B. Pieper, J. Goree, and R. A. Quinn, Phys. Rev. E **54**, 5636 (1996).
[29] D. Samsonov, J. Goree, Z. W. Ma, A. Bhattacharjee, Phys. Rev. Lett., **83**,18 (1999)
[30] G. E. Morfill et al., Phys. Rev. Lett. **83**, 1598 (1999)
[31] A. Melzer, T. Trottenberg, A. Piel, Piel Phys. Rev. E **53**, 2757 (1996)
[32] A Melzer, T. Trottenberg, A Piel, Phys. Lett. A **191**, 301-308 (1994).
[33] Lin I, Chih-Hui Chiang, J. H. Chu, Wen-Tau Jaun, Chinese Journal of Physics **33**, 5 (1995).
[34] D. Samsonov, A.V. Ivlev, R. A. Quinn, G. Morfill, S. Zhdanov, Phys. Rev. Lett. **88**, 095004 (2002).
[35] A. P. Nefedov, G. E. Morfill, V. E. Fortov, H. M. Thomas, H. Rothermel, T. Hag, A. V Ivlev, M. Zuzic, B. A. Klumov, A. M. Lipaev, V. I Molotkov, O. F Petrov, Y. P Gidzenko, S. K Krikalev, W. Shepherd, A. I. Ivanov, M. Roth, H. Binnenbruck, J. A Goree and Y. P Semenov, New J. phys. **5,** 33-1/10 (2003).
[36] C.M. Ticos, Rom. Journ. Phys., **52**(5–7), 759 (2007).
[37] B. Smith, J. Vasut, T. Hyde, L. Matthews, J. Reay, M. Cook, J. Schmoke, **34**, 2379–2383, 2381 (2004).

*Corresponding author: catalin.ticos@inflpr.ro